J Mater Sci: Mater Electron (2006) 17: 537–541
DOI 10.1007/s10854-006-8238-9

Study of electropolymerised polyaniline films using cyclic voltammetry, atomic force microscopy and optical spectroscopy

Madhulika Sharma · Diksha Kaushik · Ragini Raj Singh · R. K. Pandey

Received: 16 January 2006 / Accepted: 2 March 2006

Abstract Electropolymerisation of polyaniline (PANI) has been investigated using cyclic voltammetry in aqueous bath. The effect of dopant on the structure, morphology & optical properties of electrodeposited PANI has also been studied using x-ray diffraction (XRD), atomic force microscopy (AFM), optical absorbance & luminescence spectroscopy. It is shown that the presence of a neutral salt (KI) in the deposition matrix imparts enhanced crystallinity to PANI films.

1. Introduction

In recent years, the electrochemical synthesis of conducting polymer thin films has become an attractive interdisciplinary research field [1–3]. Conducting polymers, also known as synthetic metals, exhibit electric, electronic, magnetic and optical properties that are akin to metals or semiconductor, while the mechanical properties continue to resemble with a polymer. Amongst the known conducting polymers, polyaniline (PANI) has emerged as a promising material for future applications in molecular electronics, sensors, display devices etc, largely due to its diversity of structural forms, facile doping methodologies and a transparency in the visible region. The amorphous form of polyaniline exhibits poor interchain electron transport behavior [4]. The crystalline form of PANI salts subjected to suitable processing history in presence of dopants, show improved interchain ordering and an enhancement in the overall conductivity [5–7]. Correlation between the structure and property is currently a major area of scientific curiosity.

In this report we have investigated the electropolymerisation process for PANI in aqueous bath without or in presence of inorganic salts or dopants. The effect of the presence of the salts on the structural, morphological and optical properties of electrodeposited polyaniline have also been discussed.

2. Experimental details

Electropolymerisation of polyaniline was carried out by varying the feed ratio of monomers and dopant in aqueous electrolyte. Three different electrolyte compositions were investigated using the aqueous bath. Electrolyte I and II contained 0.1 M and 0.2 M aniline respectively in presence of 0.3 M HCl, whereas electrolyte III was prepared by adding a requisite amount of KI in electrolyte II. The electrochemical polymerization of PANI was carried out in the above three electrolytes within the potential range of -0.3 to $+1.7$ V at different scan rates using a scanning potentiostat/galvanostat model 362 (EG & G Princeton Applied Research U.S.A) under vigorous stirring at room temperature. All electrodeposition and cyclic voltammetry experiments were carried out by employing a three-electrode cell geometry comprising of a platinum counter electrode, saturated calomel (SCE) as a reference electrode and ITO or platinum foil as the working electrode. The working electrode potential was always referenced with respect to the SCE.

X-ray diffraction patterns were recorded using Shimadzu XRD-6000 diffractometer in grazing angle mode using angle

M. Sharma · D. Kaushik · R. R. Singh · R. K. Pandey (✉)
Department of Physics, Bhopal University, Bhopal 462026, India
e-mail: rkp_bu@yahoo.com
ipebu@sancharnet.in

of incidence between 0.2 to 0.3°. Cu-Kα was used as the X-ray source. The X-ray diffraction patterns were recorded between 2θ range of 15 to 30°, using the thin film attachment of the diffractometer.

The AFM experiments on electrodeposited PANI films were performed with the aid of Shimadzu SPM 9500 J2 in the contact mode.

The optical absorbance measurements were carried out at room temperature with the help of a dual beam spectrophotometer (UVPC 1601, Shimadzu) in the spectral range between 300 nm to 1100 nm; using a spectral bandwidth of 2 nm.

The photoluminescence spectra of PANI films were recorded using a computer controlled rationing Luminescence spectrophotometer LS 55 (Perkin-Elmer instrument) with λ accuracy $= \pm 1.0$ nm.

3. Results and discussions

3.1. Cyclic voltammetry

The cyclic voltammetry has been used [8–10] to study electropolymerisation of polyaniline. A number of possible pathways have been suggested for the electro-polymerization of aniline depending upon the monomer concentration, pH and nature of the dopant. The cyclic voltammetry results obtained in our studies using different set of scan rates in 0.1 M aniline & 0.3 M HCl (electrolyte I) revealed several interesting features. Typical cyclic voltammogrammes obtained using scan rate of 2 & 50 mV/sec have been shown in Fig. 1. For slower scan (2 mV/sec) we could not record any noticable peak except a sharp exponential rise of anodic current beyond +1.5 V and a weak shoulder at +1.0 V. Interestingly however, faster scan rates (50 mV/sec) revealed three oxidation peaks at lower anodic potentials and an exponential onset beyond 1.5 V. The reverse sweep also revealed two new peaks. Note that while the oxidation peaks recorded at around 0.26 & 0.45 V were not observed during slow scans the third peak at +1.0 V was earlier noticed as a weak shoulder only, while scanning at a ramp rate of 2 mV/sec. Increasing the monomer concentration in the bath to 0.2 M (electrolyte II) resulted in the cyclic voltammogramme marked as 'C' in the figure. Note that the voltammogramme 'C' resembled with 'B' except for the enhancement in the height of the peak positioned at 1.0 V. Since the oxidative peaks at 0.26 & 0.45 V were observed only at faster scan rates and also because, these are relatively unaffected by increasing monomer concentration, it is concluded that these peaks correspond to faster surface process involving aniline. It is well known that the electropolymerisation of aniline involves de-electronation and de-protonation of the monomers whose repetitive occurrence leads to the formation of polyaniline. The first two anodic peaks in the cyclic voltammogramme may, therefore be associated with these de-electronation and de-protonation steps. The peak observed at 1.0 V may be ascribed to the partial oxidation of PANI. Since the rate of electropolymerisation is expected to increase with increasing monomer concentration, the increase in height of peak at 1.0 V is in agreement with its assignment to the oxidative electropolymerisation of polyaniline. The sharp rise in the anodic current beyond 1.5 V can be assigned to complete oxidation of aniline to pernigraniline. Indeed, formation of a greenish phase was observed at approximately 1 V. During reverse scan, two peaks were observed at −0.19 V & +0.2 V as shown in Fig. 1, which correspond to the reduction of PANI.

Addition of M/50 KI in the bath resulted into significant changes in the characteristic features of the cyclic voltammogramme. Typical cyclic voltammogrammes recorded at (A) 2 mV/sec and (B) 50 mV/sec in a bath containing 0.2 M aniline, 0.3 M HCl & M/50 KI (electrolyte 3) have been shown in Fig. 2. Note that the anodic current onset recorded

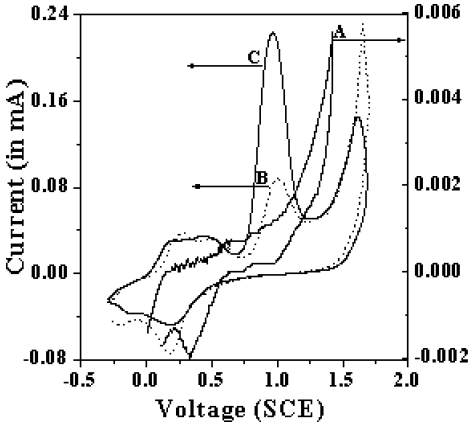

Fig. 1 Cyclic Voltammogramm recorded in electrolyte I at scan rate of (A) 2 mV/sec and (B) 50 mV/sec. Curve C was recorded in electrolyte II using a scan rate of 50 mV/sec on ITO working electrode (for details see text)

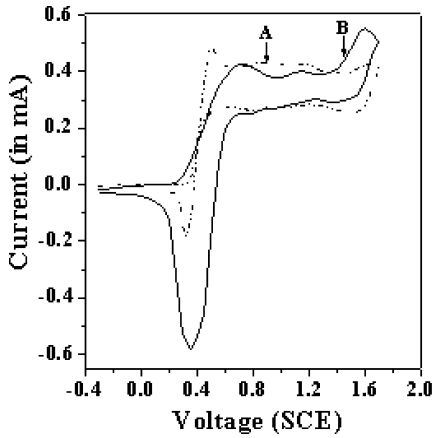

Fig. 2 Cyclic Voltammogrammes recorded in the electrolyte III at a scan rate of (A) 2 mV/sec and (B) 50 mV/sec, using ITO as the working electrode

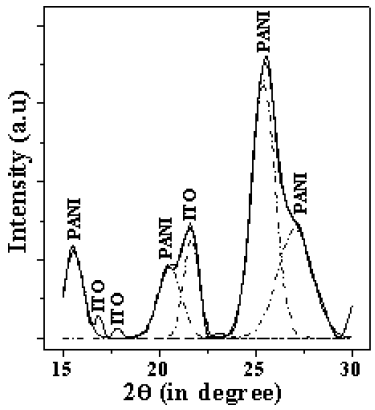

Fig. 3 Grazing angle X-Ray diffraction patterns of electrodeposited PANI film doped with HCl

at 0.33 V is more positive to the corresponding value in the absence of KI. The current is also much higher indicating increased conductivity of the bath. The anodic onset in the electrolyte 3 was quickly followed by an oxidative peak at 0.68 V and a large plateau, which later lead to a sharp exponential onset at +1.4 V. The reverse sweep revealed a sharp reduction peak at 0.35 V. A brown film was formed on the working electrode at potentials more anodic to +0.33 V. Changing the sweep rate had insignificant effect on the cyclic voltammogramme for this bath.

3.2. X-ray diffraction

Fig. 3 and 4 display the X-ray diffraction spectra of PANI samples doped with HCl and HCl + KI respectively. Note that both the XRD spectra contained the characteristic patterns of the ITO substrate also, which have been marked in the figures. The XRD spectra recorded for the HCl doped polyaniline film was marked with two weak shoulders at $2\theta = 20.52^\circ$ and 27.08°. The close proximity of the

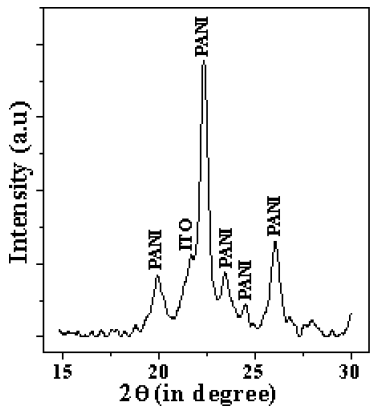

Fig. 4 Grazing angle X-Ray diffraction patterns of electrodeposited PANI film doped using HCl & KI

Table 1 A summary of the observed d-spacing and FWHM for the electrodeposited PANI

S. No	Sample History	2θ (Degree)	FWHM (Degree)	d-value (Å)
1.	HCl doped	15.53	1.21	5.70
		20.52	1.40	4.32
		25.41	1.42	3.50
		27.08	2.08	3.29
2.	HCl + KI doped	19.90	0.61	4.46
		22.35	0.47	3.62
		23.46	0.51	3.78
		24.42	0.35	3.64
		26.05	0.48	3.42

diffraction peaks along with the particle size related broadening, presumably gave rise to the observed merging of the peaks at these angular positions. To ascertain the peak positions & corresponding FWHM more accurately, these were deconvoluted assuming Gaussian lineshape, into separate peaks as shown in Fig. 3. The observed peak positions FWHM and d-spacing have been summarised in Table 1. The four diffraction peaks at $2\theta = 15.53^\circ$, 20.52°, 25.41° & 27.08° correspond to the interplanar spacing of 5.70 Å, 4.32 Å, 3.50 Å & 3.29 Å respectively, which are characteristics of the emeraldine salt phase of PANI [11]. A substantial broadening of the observed peaks was also noticed in case of HCl doped PANI. The characteristic broadening of the diffraction peaks for HCl doped PANI implied that the films are nanocrystalline. On the other hand the diffraction spectra of PANI doped with HCL + KI revealed several sharp peaks at $2\theta = 19.90^\circ, 24.42^\circ$ & 26.05°. The corresponding d-values are 4.46 Å, 3.64 Å & 3.42 Å respectively, which also agree with the d-values reported earlier [11] for the emeraldine base phase of PANI. Additionally a weak peak at $2\theta = 23.46^\circ$ corresponding to d = 3.78 Å was also seen, which was reported earlier in polyaniline salt by Winokur et al. [11]. Besides, a new strong peak was also observed at $2\theta = 22.35^\circ$ corresponding to d = 3.62 Å which was not reported earlier. Relatively sharp reflexes in the observed diffraction pattern alongwith the reduction in the observed FWHM implied increased crystallinity of PANI electrodeposited in presence of KI. The experimentally determined d values for the HCl + KI doped PANI were found to be slightly greater than the corresponding values for the HCl doped films as shown in Table 1. The d values for both the films are in good agreement with the values for emeraldine phase of PANI [11].

3.3. Atomic force microscopy

Atomic force microscopy was employed to study the morphological changes in the electrochemically deposited

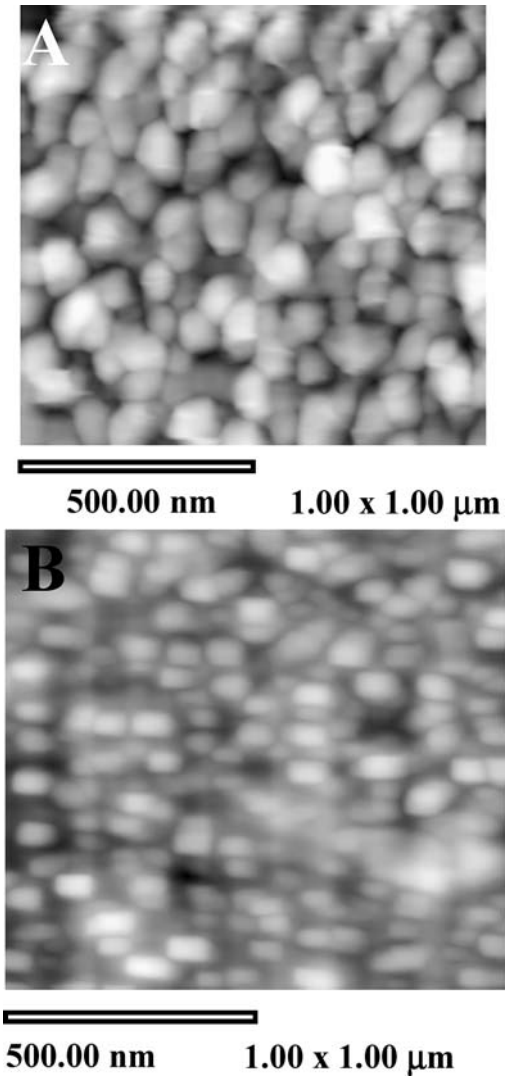

Fig. 5 Two dimensional morphology of PANI films electrodeposited in the aqueous bath in presence of (A) HCl and (B) HCl + KI

PANI films in aqueous medium in presence of different dopants. Figure 5 (A & B) represents the two-dimensional morphologies of the PANI films electrodeposited in the aqueous bath using (A) HCl and (B) HCl + KI as dopants. Note that the morphologies of HCl doped PANI is characterised by dense packing of ordered polymer bundles. The PANI bundles have an average width and length of 95.51 nm and 126.24 nm respectively. In presence of HCl & KI, the morphology of the PANI film changed significantly. The individual bundles acquire a densely packed rectangular morphology with increased ordering. The parallel ordering of polymeric bundles suggests considerable interaction between the substrate & the PANI film. The corresponding average width and length were found to be 96.85 nm and 60.16 nm.

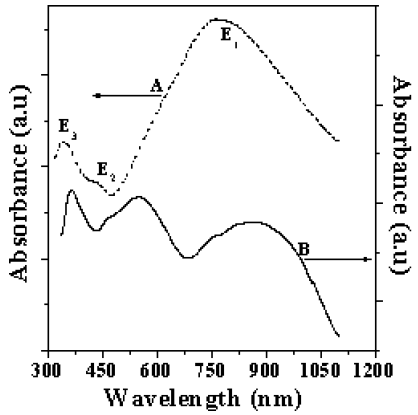

Fig. 6 Optical absorbance spectra of Polyaniline films doped with (A) HCl & (B) HCl + KI

3.4. Optical absorption spectroscopy

Figure 6 show the optical absorption spectra for PANI doped with (A) HCl & (B) HCl + KI. The HCl doped films exhibit a very broad absorption band centered at 780 nm (E_1), a weak shoulder at 437 nm (E_2) and a peak at 343 nm (E_3). On the other hand, for the HCl + KI doped PANI films the single band (E_1) recorded earlier for HCl doped film is now split into two bands centered at 850 and 550 nm. The peak centered at 550 nm is associated with the quinoid rings of the emeraldine base form of PANI [12], and is clearly resolved following KI doping. In both these bands weak shoulders at 760 and 460 nm were also recorded. Moreover, a relatively sharp absorbance peak at 360 nm was also seen which was positioned closer to the peak E_3 of the HCl doped PANI film. The absorbance bands at approximately 760 and 440 nm have been reported earlier also and may be attributed to the excitation to the polaron band [13].

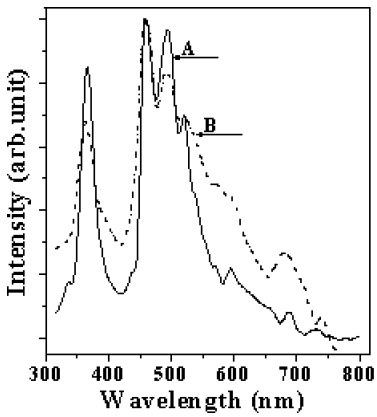

Fig. 7 Photoluminescence spectra of a typical Polyaniline film doped with (A) HCl and (B) HCl + KI

3.5. Photoluminescence spectroscopy

The photoluminescence spectra of a typical electrodeposited (A) HCl and (B) HCl + KI doped polyaniline film is shown in Fig. 7. For recording the PL spectra, the PANI film was electrodeposited on a platinum foil to avoid background contribution to the PL from the ITO substrate. The higher order contribution due to the excitation source was also subtracted from the recorded PL spectra. The PL spectrum revealed peaks at 736 nm (1.68 eV), 687 nm (1.8 eV), 595 nm (2.08 eV), 522 nm (2.37 eV), 495 nm (2.5 eV), 460 nm (2.69 eV), 366 nm (3.38 eV) and 335 nm (3.69 eV). Note that the first six PL peaks occur in the region where a broad optical absorption band was earlier recorded (see Fig. 6). It is difficult to give an unambiguous assignment to the origin of the PL peaks, due to the lack of availability of the published literature on the electronic band structure of PANI. A widely accepted model for the band structure is based on the polaron lattice model. Using a similar approach, Strafstrom et al. [13] predicted existence of lower energy transitions at (1.8 & 2.8 eV) due to the polaron bands and higher energy (4.1 eV) transitions from the upper defect band to the conduction band. Exact correlation of our PL data with the results of Strafstrom et. al. is not possible particularly since the disorder within the polyaniline structure and the presence of dopants can affect the energetic positions involved in a practical situation. However, the observation of several distinct peaks in the PL spectra indicated possibility of the existence of multiple electronic states participating in the photo-excitation process. The observed photoluminescence behaviour of PANI doped with HCl and KI also exhibited similar features as shown in Fig. 7, except that the relative intensities of all the peaks on both sides of the peak positioned at 460 nm changed.

4. Conclusion

Summarising, we have studied electrodeposition of Polyaniline in aqueous bath using HCl & KI as dopants. The oxidation and reduction peaks during electrodeposition of PANI have been well resolved by our cyclic voltammetry studies at higher scan rates. It is shown that the addition of a neutral salt KI as additive in the electrodeposition matrix imparts enhanced crystallinity to the electrodeposited film. The morphological characterisation using AFM, indicated formation of ordered bundles of polyaniline in the aqueous bath. The electrodeposited PANI films were also characterised using optical absorption and Luminescence spectroscopy. In addition to the well-known absorption bands due to polarons, a new band at 550 nm was observed following KI doping of PANI. A number of emission peak were resolved by our photoluminescence studies indicating existence of multiple electronic states including the polaron bands, defect bands and conduction band.

Acknowledgement The authors gratefully acknowledge financial support from the Department of Science and Technology, New Delhi.

References

1. F. LUX, *Polymer.* **35** (1994) 2915.
2. T. A. SKOTHEIM, in "Handbook of Conducting Polymers" (Vols I & II Marcel Dekker, New York, 1986).
3. JAN. PRZYLUSKI, "Conducting Polymer Electrochemistry" (Sci-Tech Publications, Brookfield, U.S.A 1991) p. 45.
4. Z. H. WANG, C. LI, E. M. SCHERR, A. G. MACDIARMID and A. J. EPSTEIN, *Phys. Rev. Lett.* **66** (1991) 1745.
5. M. REGHU, Y. CAO, D. MOSES and A. J. HEEGER, *Phys. Rev.* **B47** (1993) 1758.
6. A. G. MACDIARMID and A. J. EPSTEIN, *Synth. Met.* **69** (1995) 85.
7. Z. H. WANG, J. JOO, C.-H. HSU and A. J. EPSTEIN, *Synth. Met.* **68** (1995) 207.
8. W. CHEN, WENT, C. HU and A. GOPALAN, *Electrochimica. Acta.* **47** (2002) 1305.
9. M. C. BERNARD, S. JOIRET, A. H. GOFF and P. D. LONG, *J. Electrochem. Soc.* **148** (2001) B299.
10. V. RAJENDRAN, A. GOPALAN, T. VASUDEVAN and WENT, *J. Electrochem. Soc.* **147** (2000) 3014.
11. M. J. WINOKUR and B. R. MATTES, in "Conductive polymers and Plastics in Industrial applications", L. Rupprecht (Ed) (Society of Plastic Engineers, William Andrew Publishing/Plastics Design Library, 1999) p. 11.
12. B. DUKE, E. M. CONWELL and A. PATON, *Chem. Rev. Lett.* **131** (1986) 82.
13. S. STAFSTROON, J. L. BREADAS, A. J. EPSTEIN, H. S. WOO, D. B. TANNER, W. S. HUANG and A. G. MACDIARMID, *Phys. Rev. Lett.* **59** (1987) 1464.